Supporting Information (cg-2014-00039y)

Figure S1.

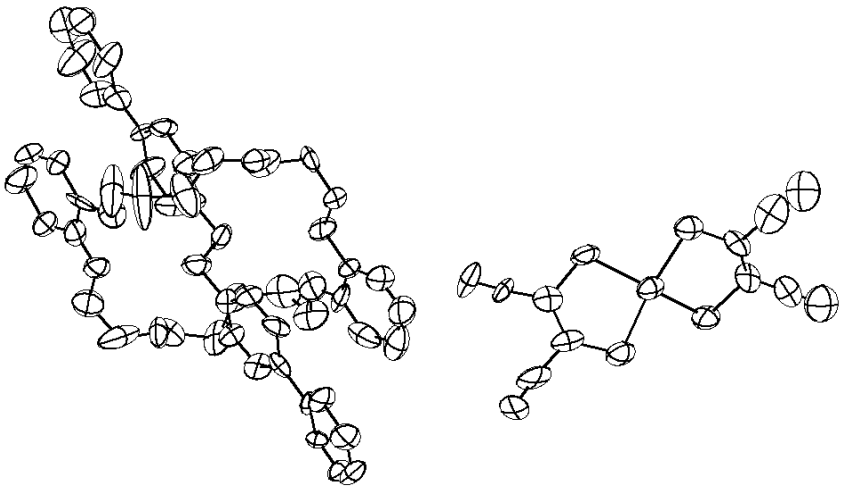

Figure S1. Thermal ellipsoid plot at the 50% probability level of the compound [Pseudorotoxane] [$Cu(mnt)_2$] (**1**). Hydrogen atoms are not shown for clarity.

Figure S2.

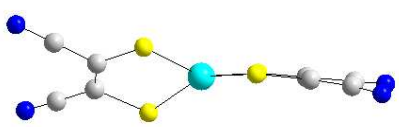

Figure S2. Distorted square planar geometry around copper ion of $[Cu(mnt)_2]^{2-}$ in compound [Pseudorotoxane] [$Cu(mnt)_2$] (**1**).

Figure S3.

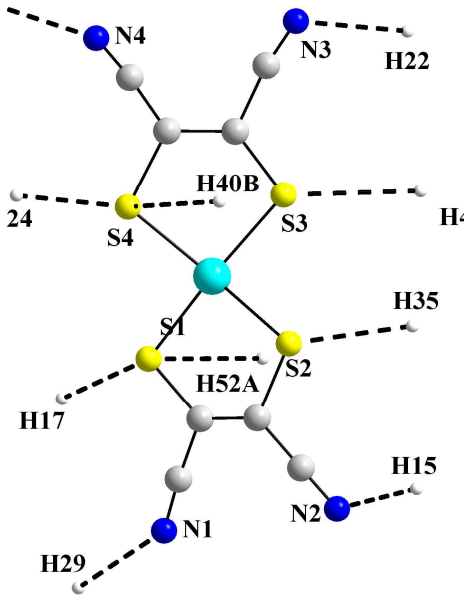

Figure S3. The involvement of $[Cu(mnt)_2]^{2-}$ anion in hydrogen bonding interactions with its surrounding.

Figure S4.

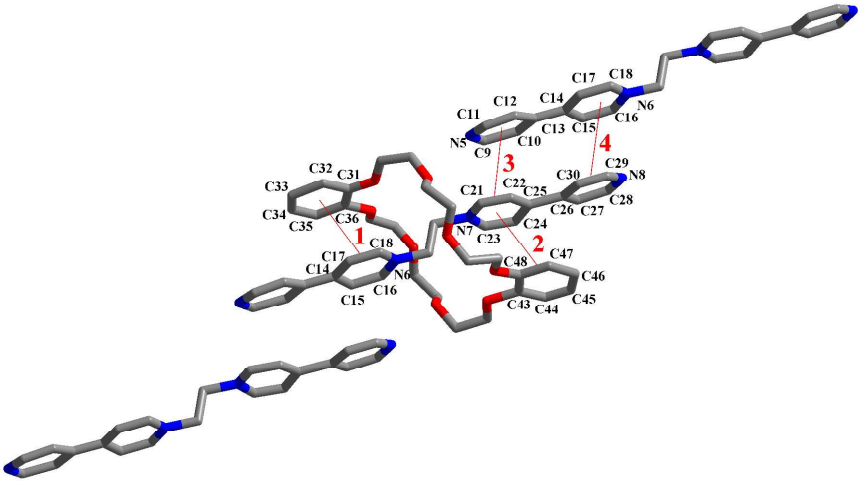

Figure S4. π-π interactions: 1: C_t–C_t = 3.728(2) Å, MPS = 3.425Å; 2: C_t–C_t = 3.788(7) Å, MPS = 3.33Å; 3: C_t–C_t = 3.679(7) Å, MPS = 3.326 Å; 4: C_t–C_t = 3.751(7) Å, MPS = 3.388 Å. C_t–C_t = centroid-to-centroid distances; MPS = mean plane separations. Color code: C, gray; N, blue; O, red.

Figure S5.

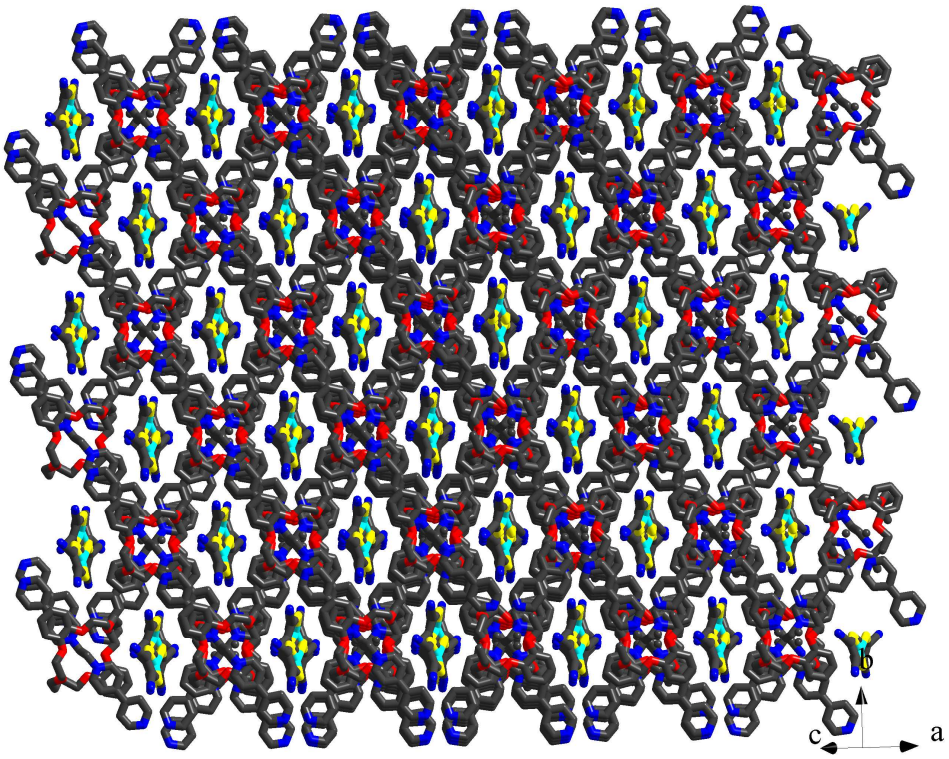

Figure S5. View (wire-frame representation) of packing diagram in the crystal structure of compound [Pseudorotoxane][Cu(mnt)$_2$] (**1**) showing well-defined void spaces that accommodate the coordination complex aions. Color code: C, gray; N, blue; O, Red; S, yellow; Cu, cyan.

Figure S6.

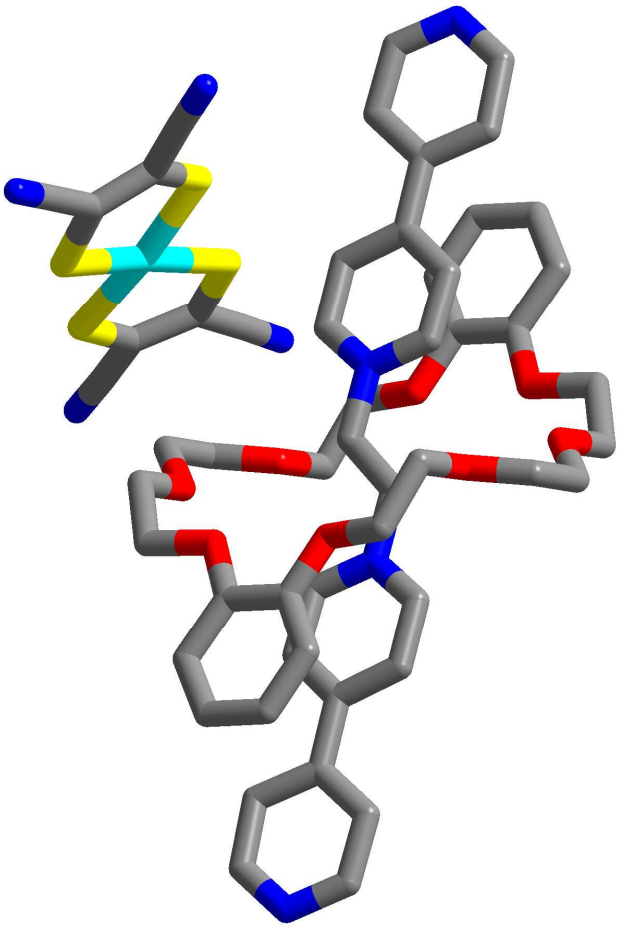

Figure S6. Molecular structure of compound **2** or **3**.

Figure S7.

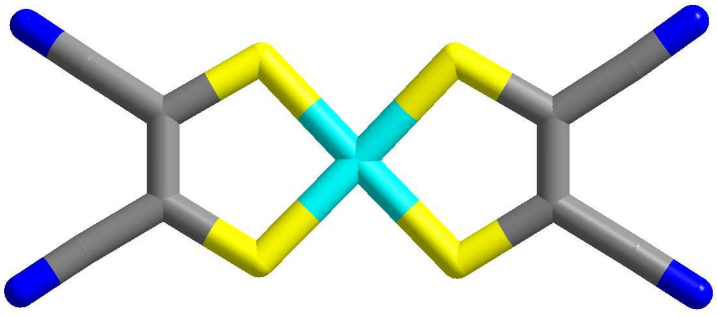

Figure S7. The existence of $[M(mnt)_2]^{2-}$ (M = Ni(II) and Pd(II)) complex anions as planar geometry in compound **2** and / or **3**.

Figure S8.

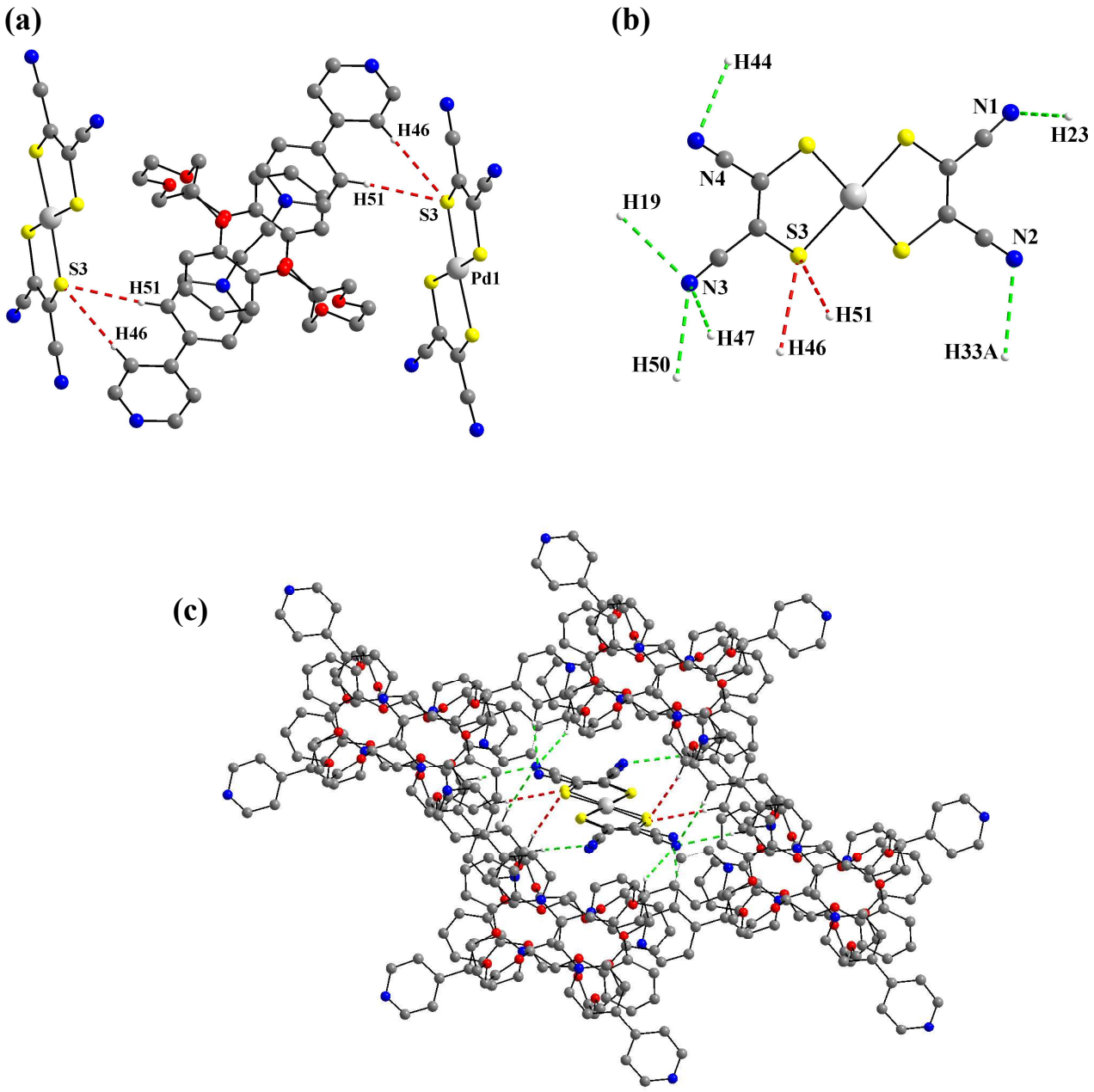

Figure S8. The C–H···X (X = S and N) hydrogen bonding interactions in **3**: (a) hydrogen bonding interaction between an $[pesudorotaxane]^{2+}$ cation and two $[Cu(mnt)_2]^{2-}$ anions; (b) the involvement of $[Cu(mnt)_2]^{2-}$ anion in hydrogen bonding and (c) hydrogen bonding interactions between an $[pesudorotaxane]^{2+}$ cation framework and two $[Pd(mnt)_2]^{2-}$ anions.

Figure S9

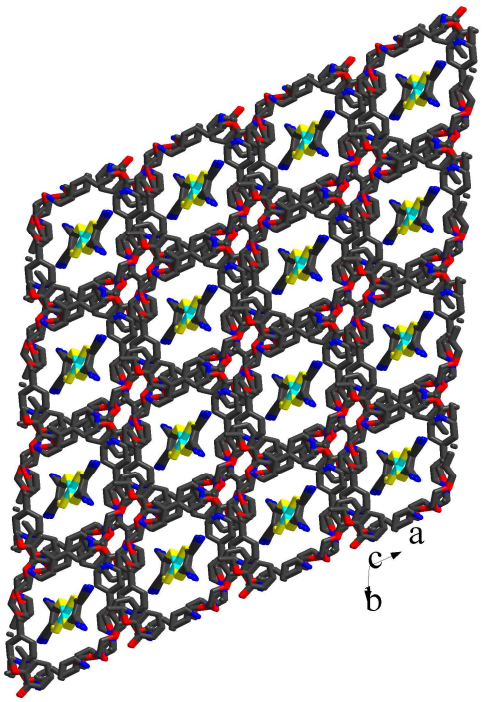

Figure S9. The view (wire-frame representation) of supramolecular architecture, formed from pseudorotaxane cations having grid type void spaces (12 Å ×12 Å) that accommodate $[M(mnt)_2]^{2-}$ (M = Ni (**2**) and Pd(**3**)) complex anions in the crystal structures of compounds **2** and **3**. Color code: C, gray; N, blue; O, Red; S, yellow; Ni or Pd, cyan

Figure S10

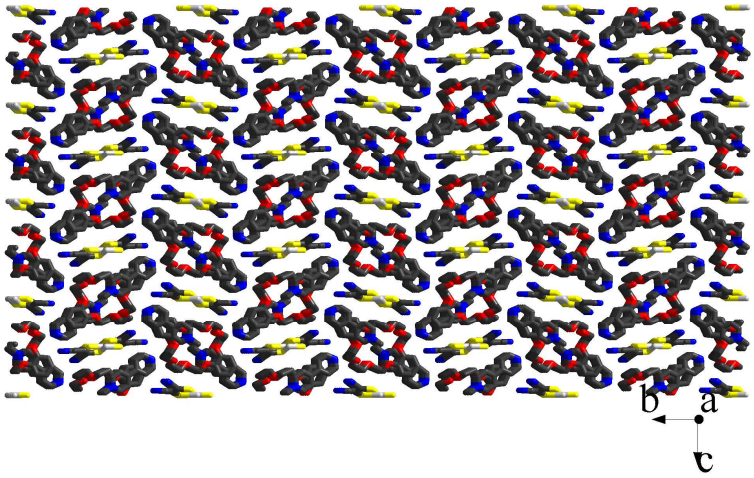

Figure S10. The view (wire-frame representation) of packing diagram in the crystal structure of compound [pseudorotaxane][$M(mnt)_2$] (**4**) displaying both $[pseudorotaxane]^{2+}$ cations and $[Pt(mnt)_2]^{2-}$ anions. Color code: C, gray; N, blue; O, Red; S, yellow; Pt, white.

Figure S11.

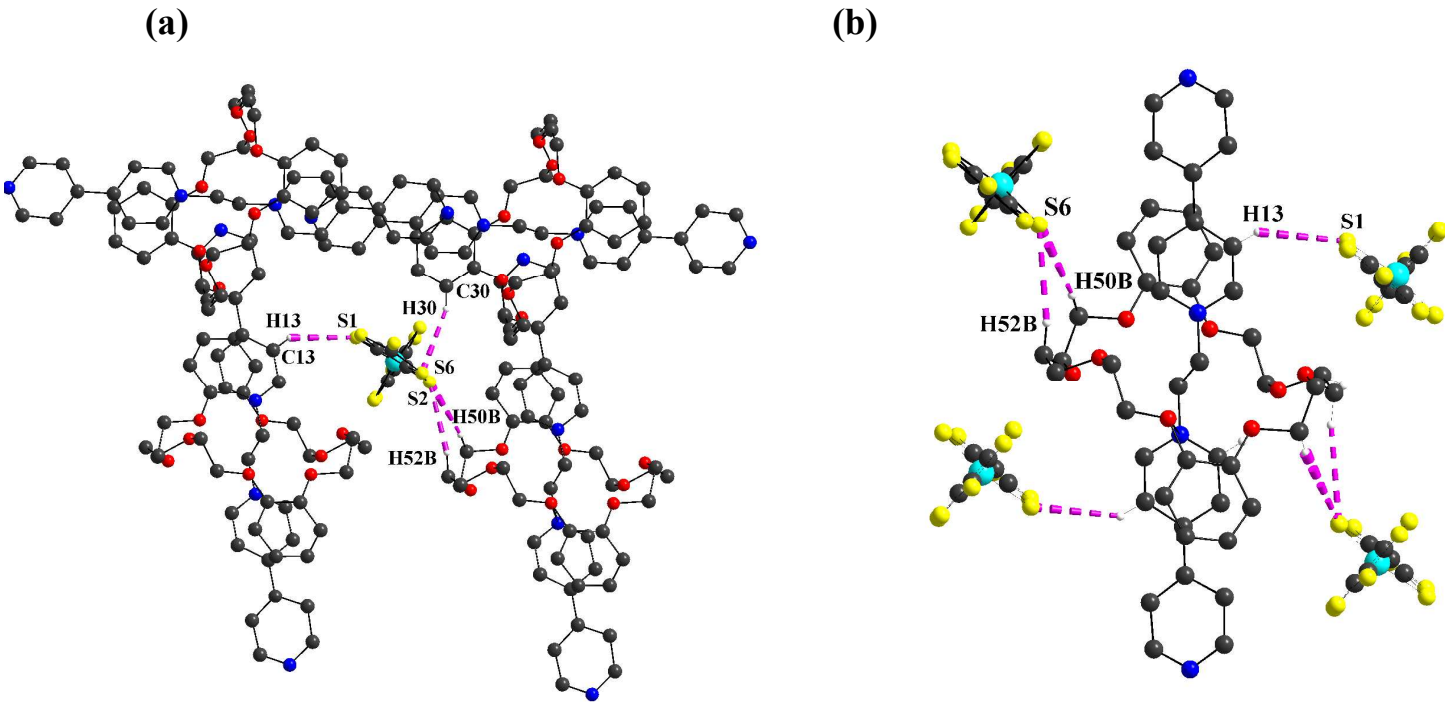

Figure S11. (a) View of the C–H···S hydrogen bonding interactions between four [pseudorotoxane] cations and one $[Zn(dmit)_2]^{2-}$ anion, (b) view of the C–H···S hydrogen bonding interactions between one [pseudorotoxane] cation and four $[Zn(dmit)_2]^{2-}$ anions in the crystal structure of compound **5**.

Figure S12.

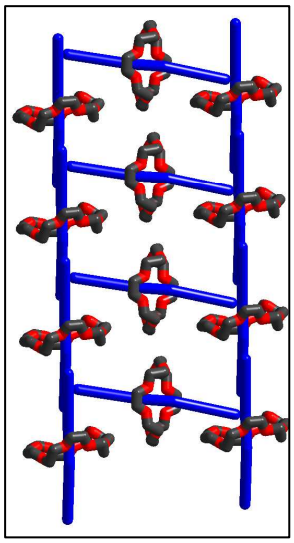

Figure S12. (a) View of molecular plane of the encapsulated $[Zn(dmit)_2]^{2-}$ complex anion, that is perpendicular to the ladder plane in the crystal of compound **5**

Figure S13

(a) (b)

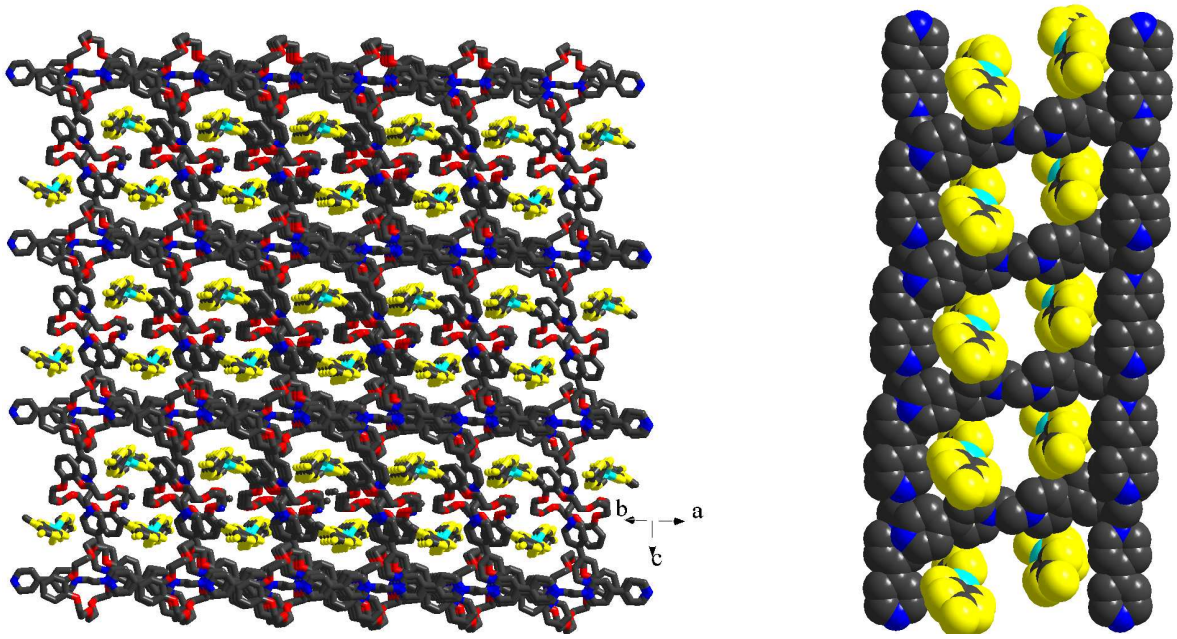

Figure S13. (a) Perspective view of ladder architectures of $[pseudorotaxane]^{2+}$ embedded with $[Zn(dmit)_2]^{2-}$ complex anions in the void spaces in compound $[pseudorotoxane][Zn(dmit)_2]$ (**5**). (b) Space filling plot of one such ladder. Color code: C, gray; N, blue; O, Red; S, yellow; Zn, cyan.

Figure S14

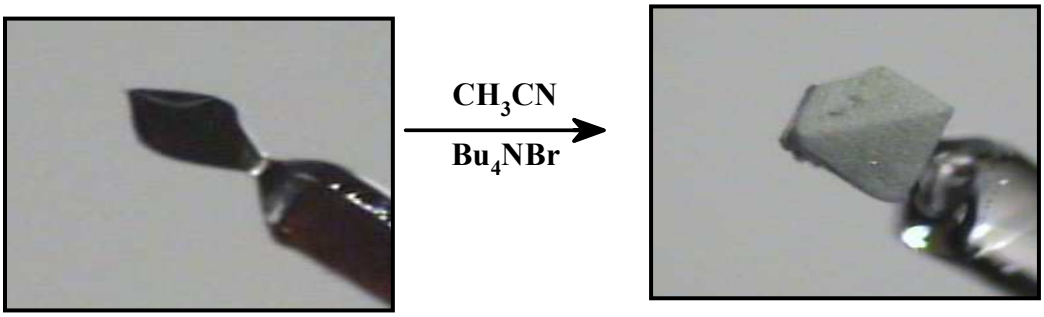

Figure S14. The dark color of the crystal $[pseudorotaxane][Cu(mnt)_2]_2$ (**1**) (left), and the color of the crystal after removing $[Cu(mnt)2]^{2-}$ anion (right) in the solid state.

Figure S15. IR spectrum

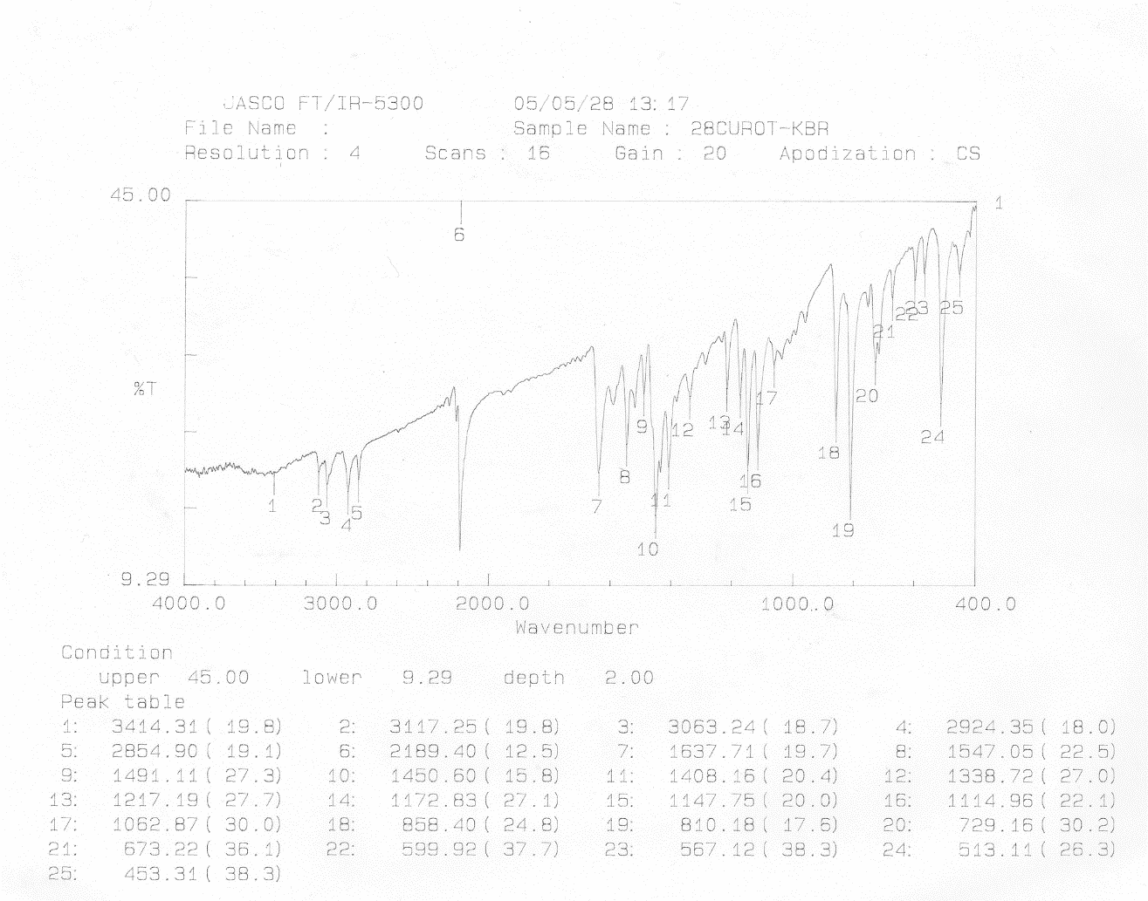

Figure S15. FTIR spectrum of [pseudorotaxane][Cu(mnt)$_2$] (**1**), which represents the IR spectra of compounds **1**□**4**.

Figure S16. IR spectrum

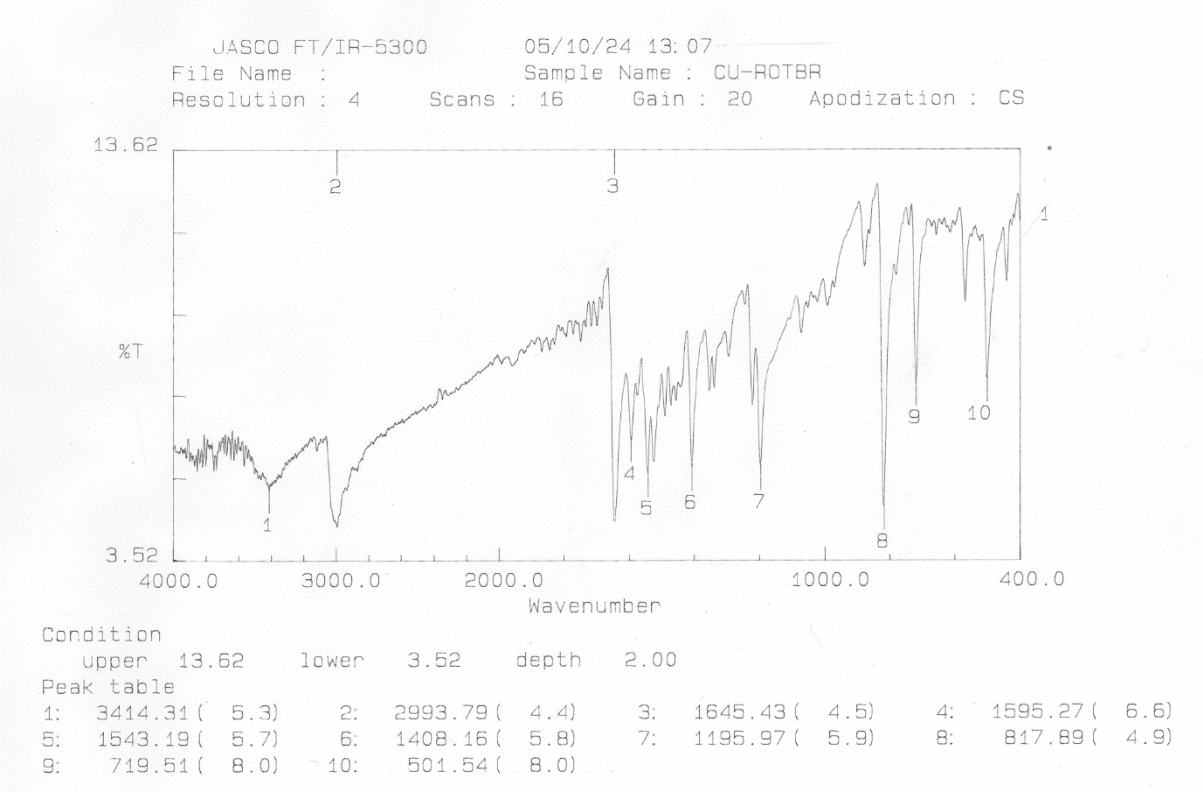

Figure S16. FTIR spectrum of [pseudorotaxane]Br_2, obtained by the reaction of [pseudorotaxane][Cu(mnt)$_2$] (**1**) in acetonitrile (compound **1** is not soluble in acetonitrile) with Bu_4NBr, dissolved in acetonitrile in a solid-liquid interface reaction.

Figure S17. PXRD patterns

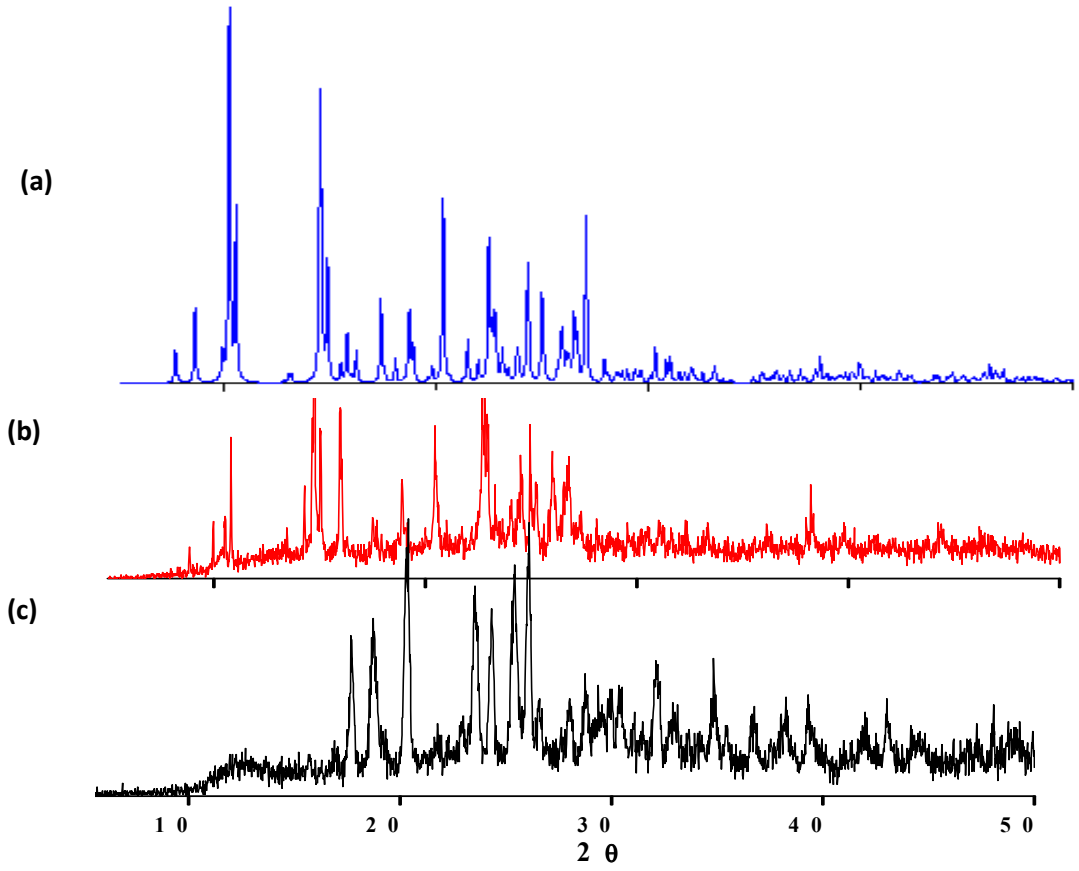

Figure S17. X-ray powder diffraction patterns: (a) simulated pattern from the crystal data of [Pseudorotaxane][$Cu(mnt)_2$] (**1**) (blue), (b) experimentally observed pattern of [Pseudorotaxane][$Cu(mnt)_2$] (**1**) (red), (c) experimentally observed pattern of [Pseudorotaxane]Br_2 (black).

Figure S18. PXRD patterns

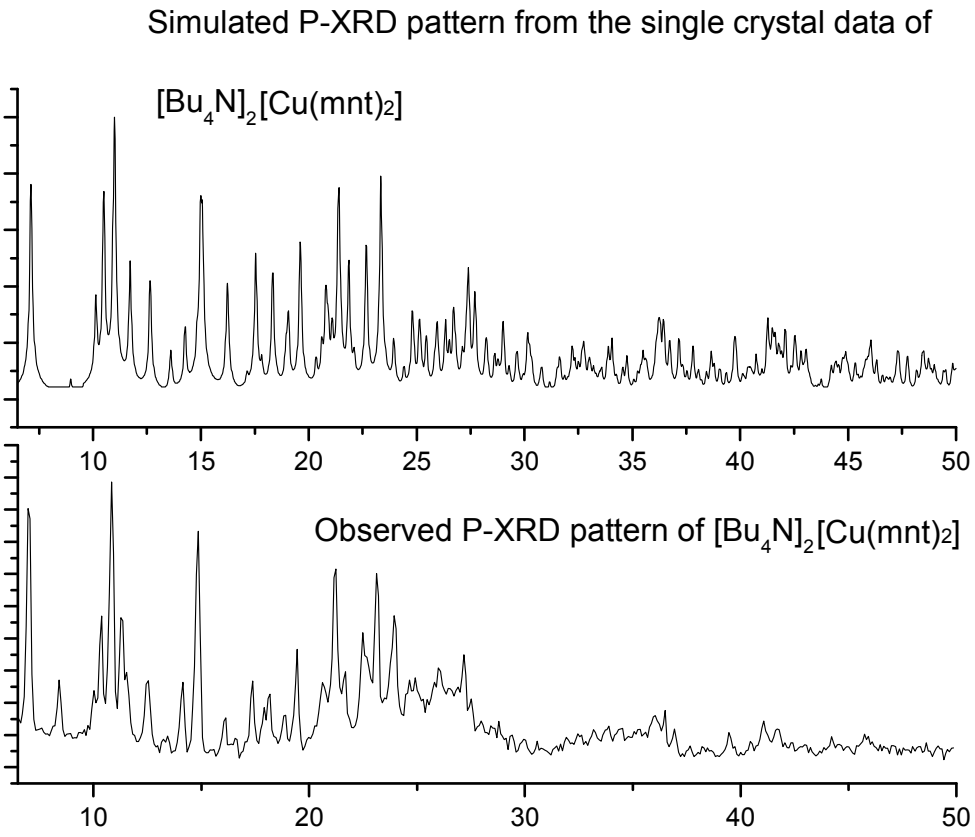

Figure S19. NMR spectrum

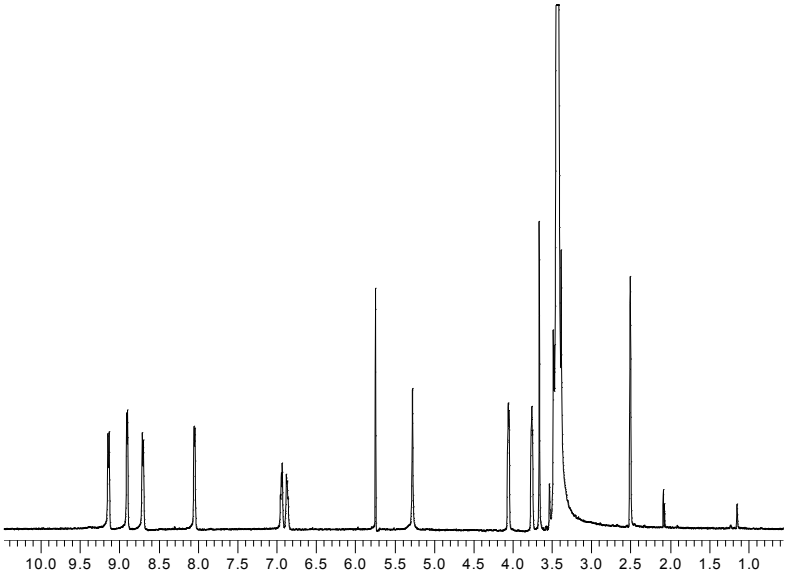

Figure S19. ^{1}H NMR spectra of (400 MHz, DMSO–d_6) of [pseudorotaxane][Ni(mnt)$_2$] (**2**) recorded at 293 K.

Figure S20. Electronic absorption spectra

(a)

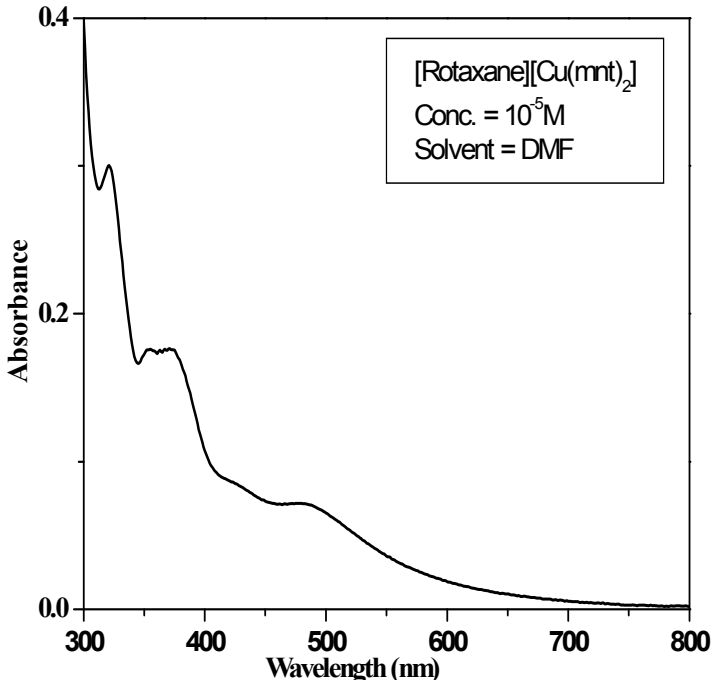

(b)

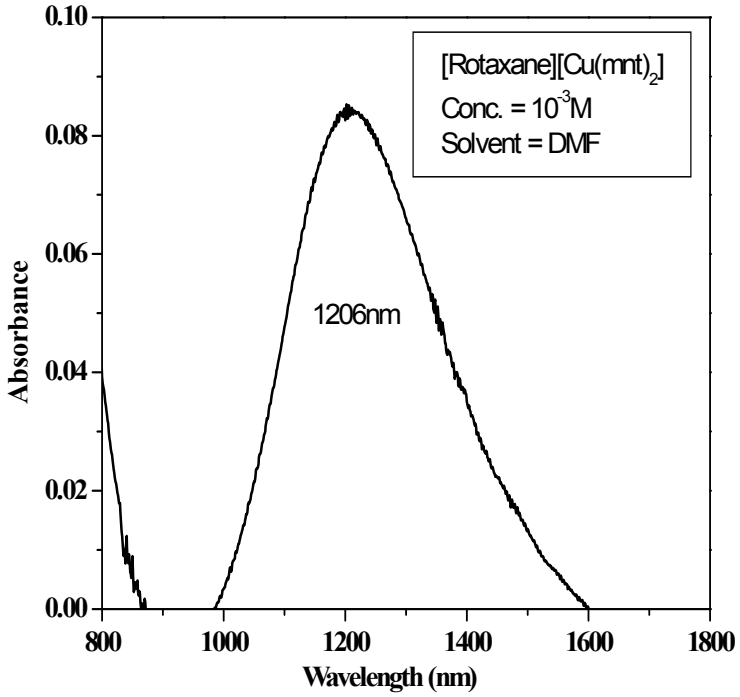
[Rotaxane][Cu(mnt)2]
Conc. = 10-3M
Solvent = DMF
1206nm
Absorbance
Wavelength (nm)
0.00
0.02
0.04
0.06
0.08
0.10
800
1000
1200
1400
1600
1800

(c)

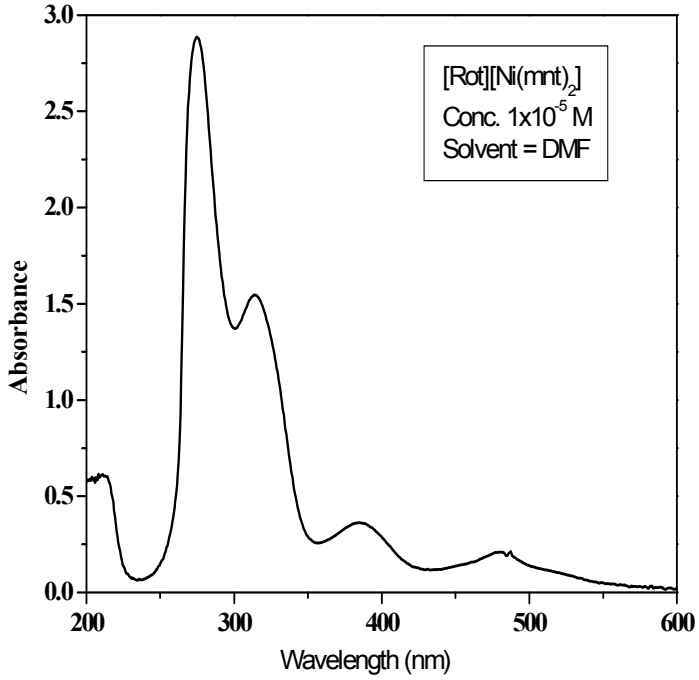
[Rot][Ni(mnt)2]
Conc. 1x10-5 M
Solvent = DMF
Absorbance
Wavelength (nm)
0.0
0.5
1.0
1.5
2.0
2.5
3.0
200
300
400
500
600

(d)

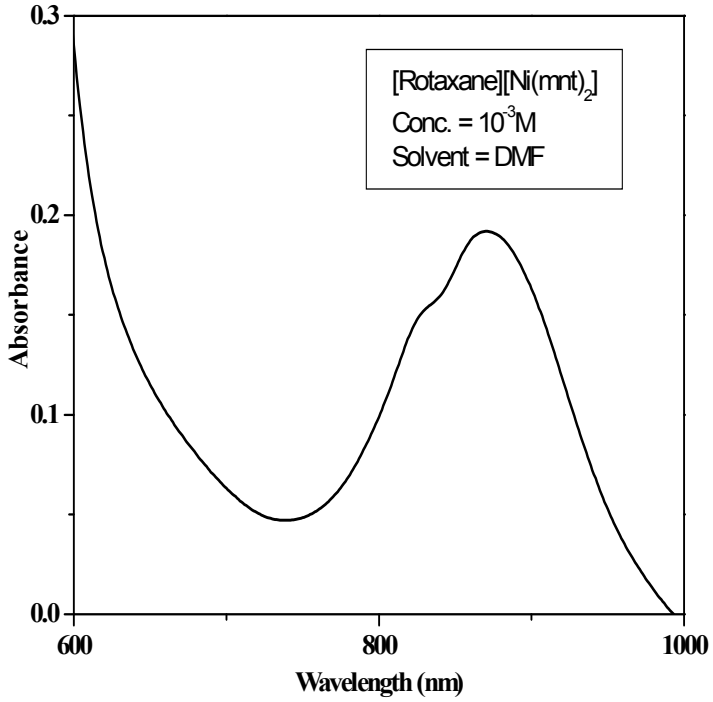
[Rotaxane][Ni(mnt)2]
Conc. = 10-3M
Solvent = DMF
Absorbance
Wavelength (nm)
0.0
0.1
0.2
0.3
600
800
1000

(e)

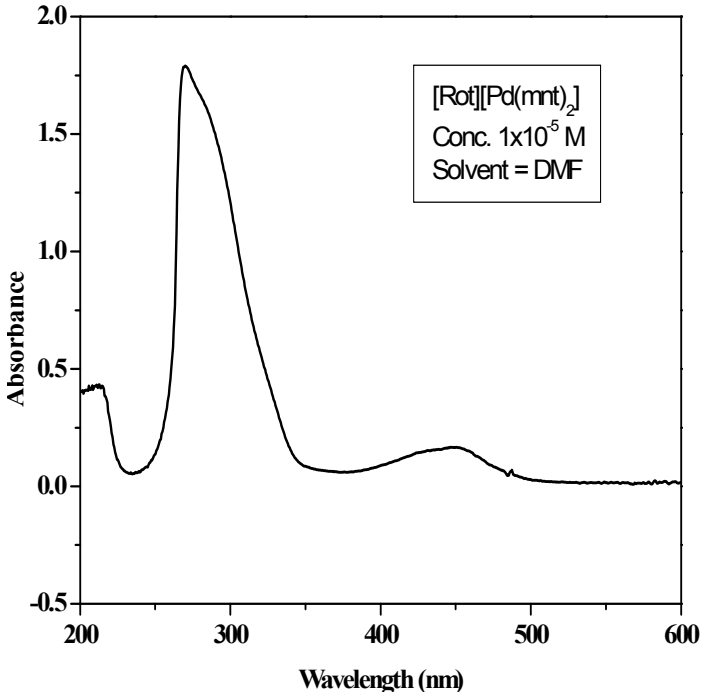
[Rot][Pd(mnt)2]
Conc. 1x10-5 M
Solvent = DMF
Absorbance
Wavelength (nm)
-0.5
0.0
0.5
1.0
1.5
2.0
200
300
400
500
600

(f)

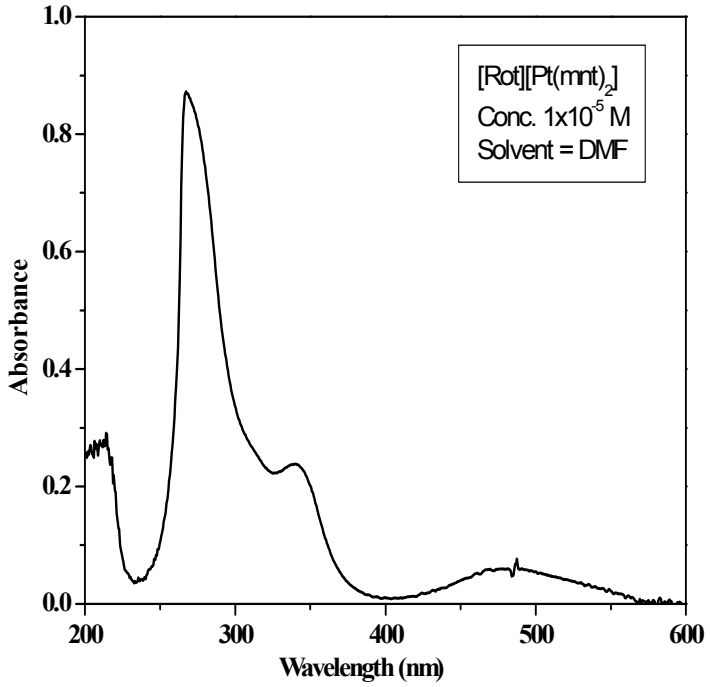

(g)

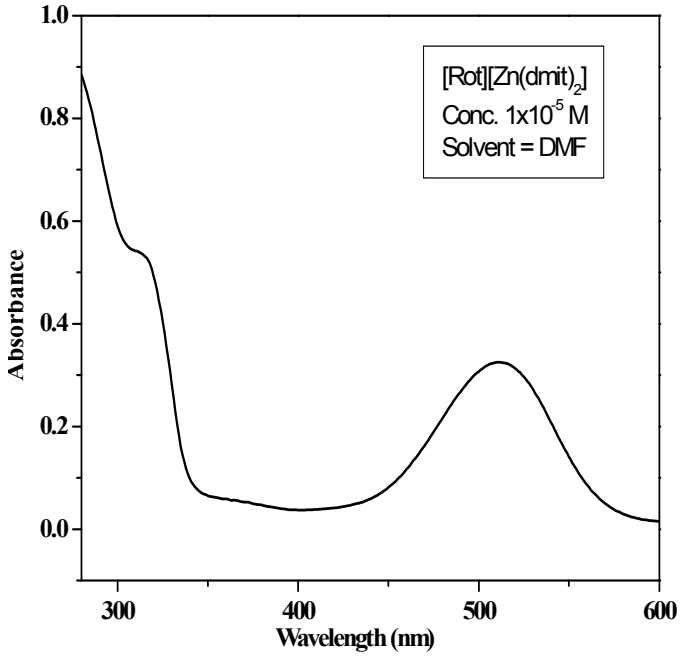

Figure S20. Electronic absorption spectra: (a) [Rotaxane][$Cu(mnt)_2$] (**1**) (1 x 10^{-5} M), (b) [Rotaxane][$Cu(mnt)_2$] (**1**) (1 x 10^{-3} M), (c) [Rotaxane][$Ni(mnt)_2$] (**2**) (1 x 10^{-5} M), (d) [Rotaxane] [$Ni(mnt)_2$] (**2**) (1 x 10^{-3} M), (e) [Rotaxane][$Pd(mnt)_2$] (**3**) (1 x 10^{-5} M), (f) [Rotaxane][$Pt(mnt)_2$] (**4**) (1 x 10^{-5} M), (g) [Rotaxane][$Zn(dmit)_2$] (**5**) (1 x 10^{-5} M) in DMF solvent at 293 K.

Figure S21. ESR spectra

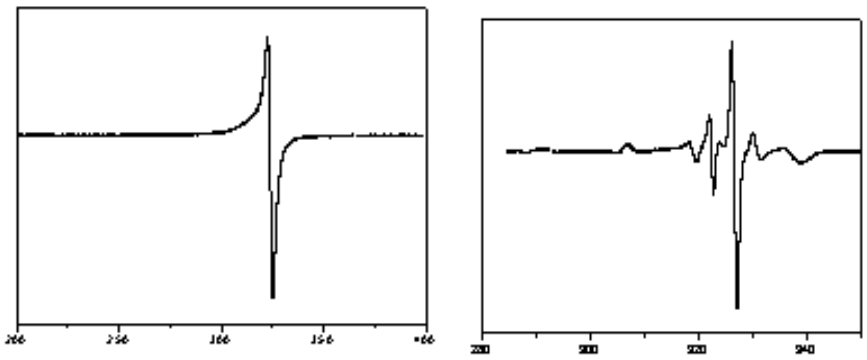

Figure S21. ESR spectrum of [pseudorotaxane][$Cu(mnt)_2$] (**1**) in solid state at room temperature (left), and ESR spectrum of **1** in DMF at liq. N_2 temperature (right).

Figure S22: NMR peaks assignment (cationic part of compound 2 as a representative example)

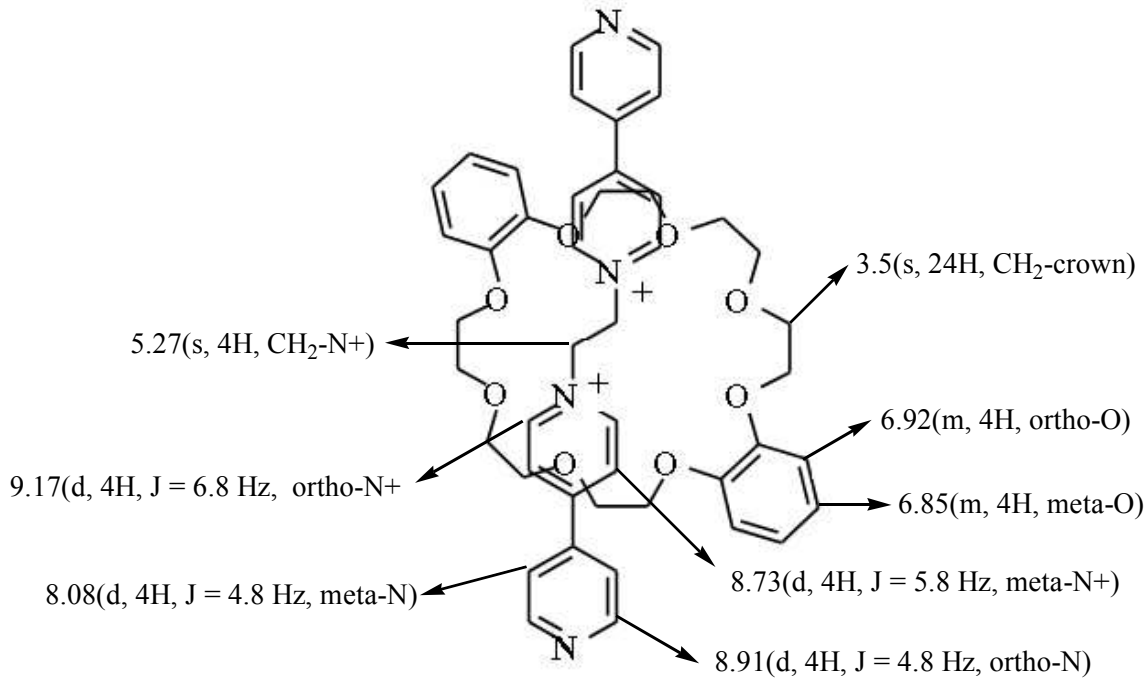

Table S1. Selected bond lengths [Å] and angles [º] for compound **1**

Cu(1)-S(1)	2.2484(13)	Cu(1)-S(2)	2.2521(14)
S(1)-C(2)	1.723(5)	S(2)-C(3)	1.730(5)
N(1)-C(1)	1.141(6)	N(2)-C(4)	1.136(6)
C(1)-C(2)	1.429(6)	C(2)-C(3)	1.347(6)
S(1)-Cu(1)-S(2)	91.32(5)	S(1)-Cu(1)-S(1)#2	94.17(7)
S(1)-Cu(1)-S(2)#2	154.91(4)	S(2)-Cu(1)-S(2)#2	94.02(8)
C(3)-S(2)-Cu(1)	100.92(17)	C(2)-S(1)-Cu(1)	101.33(16)
N(1)-C(1)-C(2)	176.0(6)	N(2)-C(4)-C(3)	175.7(6)
N(4)-C(15)-C(15)#1	110.9(4)	C(3)-C(2)-S(1)	122.6(4)
C(1)-C(2)-S(1)	116.4(3)	C(2)-C(3)-C(4)	121.5(4)
C(2)-C(3)-S(2)	123.0(4)	C(1)-C(2)-S(1)	116.4(3)
C(17)-O(1)-C(16)	115.8(4)	O(1)-C(17)-C(18)	124.2(4)

Symmetry transformations used to generate equivalent atoms: #1 -x+1/2,-y+1/2,-z+1 #2 -x+1,y,-z+1/2

Table S2. Selected bond lengths [Å] and angles [º] in the crystal structure of compound **2**

Ni(1)-S(1)	2.1585(18)	Ni(1)-S(3)	2.1599(16)
Ni(1)-S(2)	2.1642(17)	Ni(1)-S(4)	2.1707(17)
S(3)-C(5)	1.729(6)	S(4)-C(7)	1.726(6)
C(9)-O(2)	1.365(6)	C(9)-C(20)#1	1.424(7)
C(43)-O(8)	1.389(6)	C(43)-C(32)#2	1.425(8)
C(31)-C(31)#3	1.517(8)	C(44)-C(44)#4	1.517(8)
S(1)-Ni(1)-S(3)	173.07(7)	S(1)-Ni(1)-S(2)	91.91(7)
C(5)-S(3)-Ni(1)	103.4(2)	C(7)-S(4)-Ni(1)	102.7(2)
C(2)-C(1)-S(1)	117.4(5)	N(1)-C(2)-C(1)	177.2(8)
C(8)-C(7)-S(4)	117.0(5)	N(4)-C(8)-C(7)	178.8(7)

Symmetry transformations used to generate equivalent atoms: #1 -x,-y+2,-z; #2 -x+2,-y,-z+1; #3 -x,-y,-z; #4 -x,-y,-z+1.

Table S3. Selected bond lengths [Å] and angles [º] in the crystal structure of compound **3**

Pd(1)-S(3)	2.2776(15)	Pd(1)-S(1)	2.2777(16)
Pd(1)-S(2)	2.2869(16)	Pd(1)-S(4)	2.2927(16)
S(1)-C(1)	1.735(7)	S(2)-C(3)	1.725(6)
C(9)-O(2)	1.356(6)	C(9)-C(20)#1	1.410(8)
C(32)-C(43)#2	1.403(8)	C(34)-O(5)	1.434(5)
S(3)-Pd(1)-S(1)	176.11(6)	S(3)-Pd(1)-S(2)	89.45(6)
S(1)-Pd(1)-S(2)	89.94(6)	S(3)-Pd(1)-S(4)	89.94(6)
S(1)-Pd(1)-S(4)	90.91(6)	S(2)-Pd(1)-S(4)	176.29(6)
C(1)-S(1)-Pd(1)	101.9(2)	C(3)-S(2)-Pd(1)	102.1(2)
C(4)-C(3)-S(2)	115.8(5)	N(2)-C(4)-C(3)	175.0(11)

Symmetry transformations used to generate equivalent atoms: #1 -x,-y+2,-z; #2 -x+2,-y,-z+1; #3 -x,-y,-z; #4 -x,-y,-z+1

Table S4. Selected bond lengths [Å] and angles [°] in the crystal structure of compound **4**

O(14)-C(24)	1.426(4)	Pt(1)-S(2)	2.2810(8)
Pt(1)-S(2)#2	2.2811(8)	Pt(1)-S(1)#2	2.2947(8)
N(2)-C(10)	1.345(4)	N(2)-C(9)	1.345(4)
C(22)-C(27)#1	1.489(4)	C(11)-C(11)#3	1.531(6)
C(24)-O(14)-C(25)	112.1(2)	S(2)-Pt(1)-S(2)#2	180.0
S(2)-Pt(1)-S(1)#2	89.63(3)	S(2)#2-Pt(1)-S(1)#2	90.37(3)
S(2)-Pt(1)-S(1)	90.37(3)	S(2)#2-Pt(1)-S(1)	89.63(3)
S(1)#2-Pt(1)-S(1)	180.0	C(15)-S(2)-Pt(1)	102.37(11)
N(2)-C(9)-C(8)	120.4(3)	C(20)-C(16)-C(17)	119.8(3)

Symmetry transformations used to generate equivalent atoms:#1 -x+2,-y+1,-z; #2 -x+2,-y+1,-z+1; #3 -x+2,-y+1,-z+2

Table S5. Bond lengths [Å] and angles [°] in the crystal structure of compound **5**

Zn(1)-S(4)	2.321(3)	Zn(1)-S(2)	2.328(2)
Zn(1)-S(1)	2.340(2)	Zn(1)-S(3)	2.3401(18)
C(3)-S(5)	1.711(9)	C(17)-C(17)#1	1.468(14)
O(6)-C(49)	1.419(8)	C(49)-C(52)#2	1.482(11)
C(40)-C(35)#3	1.130(15)	C(10)-C(7)	1.416(13)
S(5)-C(3)-S(6)	111.5(4)	C(32)-C(31)-C(30)	123.0(8)
S(4)-Zn(1)-S(2)	115.87(10)	S(4)-Zn(1)-S(1)	116.26(9)
S(2)-Zn(1)-S(1)	94.50(7)	S(4)-Zn(1)-S(3)	95.19(8)
S(2)-Zn(1)-S(3)	117.26(7)	S(1)-Zn(1)-S(3)	119.52(7)
C(1)-S(1)-Zn(1)	96.5(2)	C(4)-S(3)-Zn(1)	95.2(2)
S(10)-C(6)-S(9)	125.6(6)	S(10)-C(6)-S(8)	123.7(6)

Symmetry transformations used to generate equivalent atoms: #1 -x+1,-y,-z+1; #2 -x+1,-y+2,-z+1; #3 -x,-y+1,-z+2

Analysis of Platon Solvent Accessible Voids in the Crystal Structures of Compounds 1-5.

Compound 1

==========

Search for and Analysis of Solvent Accessible Voids in the Structure - Grid = 0.20 Ang., Probe Radius = 1.20 Ang., NStep = 6

==========

van der Waals (or ion) Radii used in the Analysis

==========

C H Cu N O S

1.70 1.20 2.32 1.55 1.52 1.80

:: Grid: X-Axis Step = 0.0139 = Points 72, Angstrom Step = 0.20

:: Grid: Z-Axis Step = 0.0104 = Points 96, Angstrom Step = 0.20

:: Grid: Y-Axis Step = 0.0104 = Points 96, Angstrom Step = 0.21

:: Nr of VOID Grid-points = 536, - Percent Filled Space: 67.8

(See A.I. Kitajgorodskij, Molecular Crystals and Molecules, New-York, Academic Press, 1973.)

:: Total Potential Solvent Area Vol 142.2 Ang^3
per Unit Cell Vol 5368.0 Ang^3 [2.6%]

Compound 2

==========

Search for and Analysis of Solvent Accessible Voids in the Structure - Grid = 0.20 Ang., Probe Radius = 1.20 Ang., NStep = 6

==========

van der Waals (or ion) Radii used in the Analysis

==========

C H N Ni O S

1.70 1.20 1.55 2.30 1.52 1.80

:: Grid: X-Axis Step = 0.0167 = Points 60, Angstrom Step = 0.20
:: Grid: Y-Axis Step = 0.0167 = Points 60, Angstrom Step = 0.21
:: Grid: Z-Axis Step = 0.0104 = Points 96, Angstrom Step = 0.21

:: Nr of VOID Grid-points = 28, - Percent Filled Space: 67.1

(See A.I. Kitajgorodskij, Molecular Crystals and Molecules, New-York, Academic Press, 1973.)

:: Total Potential Solvent Area Vol 36.3 Ang^3
per Unit Cell Vol 2690.5 Ang^3 [1.3%]

Note: Expected volumes for solvent molecules are:
A hydrogen bonded H2O-molecule 40 Ang^3

Small molecules (e.g. Toluene) 100-300 Ang^3

Values below for gridpoints and volumes in []
refer to areas where atom centers may reside.

Compound 3

==========

Search for and Analysis of Solvent Accessible Voids in the Structure - Grid = 0.20 Ang., Probe Radius = 1.20 Ang., NStep = 6

==========

van der Waals (or ion) Radii used in the Analysis

==========

C H N O Pd S

1.70 1.20 1.55 1.52 2.30 1.80

:: Grid: X-Axis Step = 0.0167 = Points 60, Angstrom Step = 0.20
:: Grid: Y-Axis Step = 0.0167 = Points 60, Angstrom Step = 0.21
:: Grid: Z-Axis Step = 0.0104 = Points 96, Angstrom Step = 0.21

:: Nr of VOID Grid-points = 24, - Percent Filled Space: 66.9

(See A.I. Kitajgorodskij, Molecular Crystals and Molecules, New-York, Academic Press, 1973.)

:: Total Potential Solvent Area Vol 26.9 Ang^3
per Unit Cell Vol 2704.3 Ang^3 [1.0%]

Note: Expected volumes for solvent molecules are:
A hydrogen bonded H2O-molecule 40 Ang^3
Small molecules (e.g. Toluene) 100-300 Ang^3

Values below for gridpoints and volumes in []
refer to areas where atom centers may reside.

Compound 4

==========

Search for and Analysis of Solvent Accessible Voids in the Structure - Grid = 0.20 Ang., Probe Radius = 1.20 Ang., NStep = 6

==========

van der Waals (or ion) Radii used in the Analysis

==========

C H N O Pt S

1.70 1.20 1.55 1.52 2.30 1.80

:: Grid: X-Axis Step = 0.0278 = Points 36, Angstrom Step = 0.19
:: Grid: Y-Axis Step = 0.0076 = Points 132, Angstrom Step = 0.20
:: Grid: Z-Axis Step = 0.0139 = Points 72, Angstrom Step = 0.19

:: Nr of VOID Grid-points = 0, - Percent Filled Space: 72.0

(See A.I. Kitajgorodskij, Molecular Crystals and Molecules, New-York, Academic Press, 1973.)

:: Unit cell Contains NO Residual Solvent Accessible Void.

Compound 5

==========

Search for and Analysis of Solvent Accessible Voids in the Structure - Grid = 0.20 Ang., Probe Radius = 1.20 Ang., NStep = 6

==========

van der Waals (or ion) Radii used in the Analysis

==========

C H N O S Zn

1.70 1.20 1.55 1.52 1.80 2.25

:: Grid: X-Axis Step = 0.0167 = Points 60, Angstrom Step = 0.20

:: Grid: Y-Axis Step = 0.0139 = Points 72, Angstrom Step = 0.19

:: Grid: Z-Axis Step = 0.0104 = Points 96, Angstrom Step = 0.20

:: Nr of VOID Grid-points = 5331, - Percent Filled Space: 63.6

(See A.I. Kitajgorodskij, Molecular Crystals and Molecules, New-York, Academic Press, 1973.)

:: Total Potential Solvent Area Vol 270.9 Ang^3
per Unit Cell Vol 2989.2 Ang^3 [9.1%]

*******************End of Supporting Information*******************